Multi-Target Tracking with Unattended Ground Sensors (UGS) Data

Stefano Coraluppi, Craig Carthel, and Mahendra Mallick
ALPHATECH, Inc.
50 Mall Rd, Burlington, MA 01803
{stefano.coraluppi,craig.carthel,mahendra.mallick}@alphatech.com
Tel. +1-781-273-3388 ext. 366
Fax: +1-781-273-9345

ABSTRACT

This paper studies the performance of an Extended Kalman Filter/Multi-Hypothesis Tracking (EKF/MHT) approach to target tracking with data from seismic and acoustic sensors. We study the impact on tracking performance of the number, placement, and detection threshold associated with these sensors. Our algorithm scales well as the number of sensors increases, indicating its suitability for processing data sets associated with large numbers of unattended ground sensors.

Keywords: Multi-Sensor Multi-Target Tracking, Unattended Ground Sensors (UGS), Acoustic Sensors, Seismic Sensors

1. INTRODUCTION

Track-oriented multi-hypothesis tracking is a powerful yet computationally intensive approach to target tracking [1]. Early work on this technology at ALPHATECH is documented in [2]. Recently, we have extended the approach to handle detection-level as well as track-level data, with hypothesis selection based on a computationally efficient LP-relaxation approach [3][4]. In this paper, we extend the approach further to include bearings-only data, allowing for the efficient processing of data from acoustic and seismic unattended ground sensors (UGS). We study the performance of our tracking algorithm as a function of the number, placement, and detection threshold associated with these sensors. Finally, we identify key issues and promising approaches for further research in UGS tracking.

2. TARGET MODELS, SENSOR MODELS, AND EKF/MHT PROCESSING

Evasive target motion can be represented with a number of stochastic dynamical models of varying complexity. The simplest such model is a Markovian stochastic process that is linear and has independent additive Gaussian noise. This is the *nearly constant velocity model* (NCVM):

$$\dot{X}(t) = F(t)X(t) + w(t), \tag{2.1}$$

$$X(t) = \left[x(t) \quad y(t) \quad \dot{x}(t) \quad \dot{y}(t)\right]', \tag{2.2}$$

$$F(t) = \begin{bmatrix} 0 & 0 & 1 & 0 \\ 0 & 0 & 0 & 1 \\ 0 & 0 & 0 & 0 \\ 0 & 0 & 0 & 0 \end{bmatrix}, \tag{2.3}$$

$$w(t) = \left[0 \quad 0 \quad w_x(t) \quad w_y(t)\right]', \tag{2.4}$$

where $w_x(\cdot)$ and $w_y(\cdot)$ are mutually independent, zero-mean white Gaussian processes with $E\left[w_x(t)w_x(\tau)\right] = q_x\delta(t-\tau)$ and $E\left[w_y(t)w_y(\tau)\right] = q_y\delta(t-\tau)$. Targets have an unknown initial position, and the probability distribution for initial target velocity given by:

$$\begin{bmatrix} \dot{x}(0) \\ \dot{y}(0) \end{bmatrix} \sim N(0, \Sigma_I). \tag{2.5}$$

Report Documentation Page

Report Date	Report Type	Dates Covered (from... to)
00 Oct 2001	N/A	-

Title and Subtitle Multi-Target Tracking with Unattended Ground Sensors (UGS) Data	**Contract Number**
	Grant Number
	Program Element Number
Author(s)	**Project Number**
	Task Number
	Work Unit Number
Performing Organization Name(s) and Address(es) ALPHATECH, Inc 50 Mall Rd Burlington, MA 01803	**Performing Organization Report Number**
Sponsoring/Monitoring Agency Name(s) and Address(es) Department of the Army, CECOM RDEC Night Vision & Electronic Sensors Directorate AMSEL-RD-NV-D 10221 Burbeck Road Ft. Belvoir, VA 22060-5806	**Sponsor/Monitor's Acronym(s)**
	Sponsor/Monitor's Report Number(s)

Distribution/Availability Statement
Approved for public release, distribution unlimited

Supplementary Notes
See also ADM201471, Papers from the Meeting of the MSS Specialty Group on Battlefield Acoustic and Seismic Sensing, Magnetic and Electric Field Sensors (2001) Held in Applied Physics Lab, Johns Hopkins Univ, Laurel, MD on 24-26 Oct 2001. Volume 2 (Also includes 1999 and 2000 Meetings), The original document contains color images.

Abstract

Subject Terms

Report Classification unclassified	**Classification of this page** unclassified
Classification of Abstract unclassified	**Limitation of Abstract** UU

Number of Pages
10

Sensor observations associated with the ground target are defined at a sequence of non-decreasing times $t_k \in (t_1, t_2, ...)$. Discretization of the continuous-time dynamics based on this sequence of times yields the following:

(2.6) $$X_{k+1} = \Phi_k X_k + w_k ,$$

(2.7) $$X_k = \begin{bmatrix} x_k \\ y_k \\ \dot{x}_k \\ \dot{y}_k \end{bmatrix} = \begin{bmatrix} x(t_k) \\ y(t_k) \\ \dot{x}(t_k) \\ \dot{y}(t_k) \end{bmatrix},$$

(2.8) $$\Phi_k = \begin{bmatrix} 1 & 0 & \Delta t_k & 0 \\ 0 & 1 & 0 & \Delta t_k \\ 0 & 0 & 1 & 0 \\ 0 & 0 & 0 & 1 \end{bmatrix}, \ \Delta t_k = t_{k+1} - t_k ,$$

and $\{w_k, k \geq 1\}$ is a zero-mean white Gaussian process, and $w_k \sim N(0, Q_k)$ with

(2.9) $$Q_k = \begin{bmatrix} \frac{1}{3} q_x (\Delta t_k)^3 & 0 & \frac{1}{2} q_x (\Delta t_k)^2 & 0 \\ 0 & \frac{1}{3} q_y (\Delta t_k)^3 & 0 & \frac{1}{2} q_y (\Delta t_k)^2 \\ \frac{1}{2} q_x (\Delta t_k)^2 & 0 & q_x \Delta t_k & 0 \\ 0 & \frac{1}{2} q_y (\Delta t_k)^2 & 0 & q_y \Delta t_k \end{bmatrix}.$$

Note that we have defined target trajectories to lie on the *xy*-plane. A three-dimensional state will be required in certain applications; in ground target tracking, the *z* coordinate is often a known function of the target location on the *xy*-plane. Numerous generalizations to our simple model exist, including Gauss-Markov process noise models, hybrid-state models, and more general, nonlinear stochastic models [5]. Also, it may be the case that model parameters, particularly the intensity of the process noise, are unknown and must be estimated as well. Perhaps the most popular recent generalization is to use hybrid-state models, for which the *Interacting Multiple Model* (IMM) filter [6] is an efficient recursive nonlinear filter that generalizes the well-known *Extended Kalman Filter* (EKF).

As with target models, sensor models may have varying levels of complexity. We assume that measurements are a nonlinear function of the target state X_k and the sensor state $\overline{X}_k$, with an additive independent Gaussian noise process $\{v_k, k \geq 1\}$. That is:

(2.10) $$Y_k = h(X_k, \overline{X}_k) + v_k, v_k \sim N(0, R_k),$$

(2.11) $$\overline{X}_k = \begin{bmatrix} \bar{x}_k & \bar{y}_k & \dot{\bar{x}}_k & \dot{\bar{y}}_k \end{bmatrix}'.$$

Note that the dimension of the measurement Y_k will depend on the sensor.

Our experimental results will be based on simulated detections from acoustic and seismic ground sensors. Our kinematic measurement models are as follows. For acoustic data, we have:

(2.12) $$h(X_k, \overline{X}_k) = \tan^{-1}(x_k - \bar{x}_k, y_k - \bar{y}_k).$$

For seismic data, we have:

(2.13) $$h(X_k, \overline{X}_k) = \begin{bmatrix} \left((x_k - \bar{x}_k)^2 + (y_k - \bar{y}_k)^2\right)^{0.5} \\ \tan^{-1}(x_k - \bar{x}_k, y_k - \bar{y}_k) \end{bmatrix}.$$

We will assume that the area of interest is small and relatively flat, so that a second angular measurement from the sensors is not necessary, i.e. we restrict attention to 2D scenarios. We assume that the sensing range and measurement precision are known for all sensors. All sensors are characterized by a sensor-dependent probability of detection p_D and a false alarm rate. In particular, we assume that the number of false alarms per scan of data per unit area obeys a Poisson distribution with a sensor-dependent parameter λ_{FA}, and the false alarms are uniformly distributed in the region of regard of the sensor.

In addition to a kinematic state, in general targets may also be characterized by a discrete state, or feature state. A sensor-dependent classification confusion matrix characterizes feature measurements. Low-confusion feature measurements can be crucial in effective tracking in high target density environments. For the purposes of the analysis in this paper, we will not be considering feature measurements in seismic and acoustic data.

Given the nonlinear observation equations (2.10)-(214), we use a standard EKF approach to recursive estimation of the kinematic state associated with each track hypothesis. This is a straightforward approach and is briefly summarized below for completeness. We denote by $X(k \mid k)$ and $P(k \mid k)$ the conditional mean and covariance for the kinematic state of a track at time t_k, given all information up to and including time t_k. Also, we denote by $X(k+1 \mid k)$ and $P(k+1 \mid k)$ the predicted mean and covariance for the kinematic state of a target at time t_{k+1}, given all information up to and including time t_k. The initial position estimate is given by a maximum likelihood estimate. Subsequently, we proceed as follows.

(2.14) $$X(k+1 \mid k) = \Phi(\Delta t_k) X(k \mid k),$$

(2.15) $$P(k+1 \mid k) = \Phi(\Delta t_k) P(k \mid k) \Phi'(\Delta t_k) + Q(\Delta t_k),$$

(2.16) $$X(k+1 \mid k+1) = X(k+1 \mid k) + L(k+1)\left(Y_{k+1} - h\left(X(k+1 \mid k), \overline{X}_k\right)\right),$$

(2.17) $$P(k+1 \mid k+1) = (I - L(k+1)C(k+1))P(k+1 \mid k),$$

(2.18) $$L(k+1) = P(k+1 \mid k)C'(k+1)\left(C(k+1)P(k+1 \mid k)C'(k+1) + R_k\right)^{-1}$$

(2.19) $$C(k+1) = \left.\frac{\partial h\left(X_{k+1}, \overline{X}_{k+1}\right)}{\partial X_{k+1}}\right|_{X_{k+1} = X(k+1|k)}.$$

A key component in target tracking algorithms is the solution to the data association problems. We refer the reader to the details of our MHT approach described in [3][4]. Additional approaches, including the PMHT and JPDA are described in [1] and references therein. The following is a summary of modifications to our EKF/MHT algorithm for processing bearing-only data.

- In the case of an acoustic measurement, set range measurement to 2/3 the sensing range of the sensor, with a very large range measurement variance[1].
- Use an angle-only gating mechanism in generating track-to-measurement associations with acoustic measurements.
- Introduce a second gating mechanism, whereby associations that lead to a kinematic update that falls outside the bounding circle of the current sensor are rejected. (This significantly reduces ghosting effects [1].)
- Only report tracks with a sufficiently small estimation covariance, ensuring that two distinct sensors are involved in each track displayed. Typically, this removes the initial segment of some tracks and will remove those tracks associated with a single sensor.
- Secondary likelihood calculations relevant to track termination are maintained on all track *coasts* (track continuations with no sensor measurement).

Note that, as with other sensor types, acoustic and seismic data are characterized by detection probabilities and false alarm rates. Currently, our track likelihood calculations do not depend on these quantities. Detection probabilities and false alarm rates are used implicitly by appropriately modifying the following algorithm parameters.

---

[1] A natural choice for the initial range estimate given uniformly likely target location and a sensor range of r_S is as follows:

$$\hat{r} = \frac{1}{\pi r_S^2} \int_{\text{Area}} r\,dx\,dy = \frac{1}{\pi r_S^2} \int_0^{2\pi} \int_0^{r} r \cdot r\,dr\,d\theta = \frac{2}{3} r_S .$$

- *Confirmation threshold*. Rather than using an explicit track initiation scheme, e.g. SPRT [1], we use a post-processing step that removes tracks that do not satisfy a lower bound on the time duration of the track.
- *Termination threshold*. This threshold, to which secondary likelihoods are compared, determines how long a track may coast before it is terminated. Note that the same threshold is applied to all active tracks, whether or not they are ultimately confirmed. Other approaches have been considered in the literature [1][2].

Note that our approach to processing passive sensor data has not required use of modified polar or spherical coordinates [1][7][8]. Indeed, due to the multi-sensor nature of our problem, it is more convenient to consider a single, Cartesian coordinate system for centralized tracking.

3. EXPERIMENTAL FRAMEWORK

Our experimentation is based on a MATLAB-based infrastructure for data simulation and performance evaluation, and a C++ based executable that constitutes the key EKF/MHT functional component. Data simulation includes the following components:

- *Ground Truth Simulation*. We generate stochastic realizations of target motion for an arbitrary number of targets, according to a NCVM model for target motion. Targets are restricted to move in a region of fixed size by reflecting their motion back into the region when they move outside. Motion is restricted to a two-dimensional *xy* plane. Simulation parameters are listed in Table 3.1.

Scenario length	60s
Process noise parameter in x-direction, q_x	$0.01\text{m}^2\text{sec}^{-3}$
Process noise parameter in y-direction, q_y	$0.01\text{m}^2\text{sec}^{-3}$
Size of region for target motion	$(300\text{m})^2$
Target velocity covariance prior	$\begin{bmatrix} 1 & 0 \\ 0 & 1 \end{bmatrix} \left(\text{m}/\text{sec}\right)^2$

Table 3.1. Ground truth simulation parameters.

- *Sensor data simulation.* The type of sensor (acoustic and/or seismic), as well as the number, location, detection probability and false alarm rates are the key data simulation parameters that we will vary. Other parameters are listed in Table 3.2.

Data rate for seismic sensors	1Hz
Data rate for acoustic sensors	2Hz
Range measurement covariance for seismic sensors	100m^2
Azimuth measurements covariance for seismic sensors	$(0.05236\text{Rad})^2 = (3\,\text{deg})^2$
Azimuth error covariance for acoustic sensors	$(0.05236\text{Rad})^2 = (3\,\text{deg})^2$
Seismic sensor range	250m
Acoustic sensor range	750m

Table 3.2. Sensor data simulation parameters.

- *Key EKF/MHT algorithm parameters*. We will vary the confirmation threshold. The association gates, termination thresholds, and depth for the set of hypothesis trees are listed in Table 3.3.

Seismic data association gate multiplier	9.210 (99% confidence)
Azimuth gate for acoustic measurements	$18\,\text{deg}$
Termination threshold	1sec
Depth of hypothesis trees	4

Table 3.3. Tracking algorithm parameters.

- *Performance Metrics*. There is no single performance measure that quantifies the quality of a tracking algorithm. Typically, one must trade off tracking performance with respect to a number of metrics of interest. Table 3.4 lists the performance metrics that we consider, along with a brief description. Additional comments are given below.

Computation time	Total processing time [sec]
Percentage of false tracks	Fraction of tracks classified as false
Fragmentation	Ratio of number of confirmed tracks and number of targets
Probability of correct association	Ratio of total number of correct associations and total number of associations in tracks classified as true
Track life	Ratio of total duration of true tracks and total duration of target trajectories
Scan-by-scan position RMSE	RMSE position error for true tracks, computed by associating each state estimate to the target which last contributed a report to the track [m]
Scan-by-scan velocity RMSE	RMSE velocity error for true tracks, computed by associating each state estimate to the target which last contributed a report to the track [m/sec]
Global-mapping position RMSE	RMSE position error for true tracks, computed on the basis of a track to target association [m]
Global-mapping velocity RMSE	RMSE velocity error for true tracks, computed on the basis of a track to target association [m/sec]

Table 3.4. Performance metrics for tracking.

Several of the metrics listed above depend on the classification of each track as *false* or *true*, and, in the latter case, on an association of each track to a target. The classification is based on identifying the target that contributed to the most sensor measurements utilized in forming a track. If a track includes more false measurements than measurements originating from any single target, the track is classified as *false*. The fraction of false tracks is an important metric that reflects the reliability of confirmed tracks. False tracks are included in the *fragmentation* computation, yet they are discarded in the *track life* and *RMSE* computations.

The issue of how best to evaluate the position and velocity *RMSE* associated with tracks that we classify as *true* is a non-trivial one. Consider the following example, in which two targets lead to a set of measurements in clutter, which are then processed into a set tracks. Assume that one of these track has a life over 7 scans, and contains 4 sensor measurements. The tracks is as follows:

Scan #	Origin of measurement	Scan-by-scan classification
Scan 1	Measurement from target 1	Target 1
Scan 2	Track coast (i.e. no measurement)	Target 1
Scan 3	False measurement	Target 1
Scan 4	Measurement from target 1	Target 1
Scan 5	Measurement from target 2	Target 2
Scan 6	Track coast	Target 2
Scan 7	Track coast	Target 2

Table 3.5. RMSE computation example.

First, note that the target than contributes the most measurements to the track is target 1. Since there are two such measurements, and only one false measurement, the track is classified as *true* and is associated with target 1. For *the global-mapping position and velocity RMSE*, we compare the track estimates the actual position and velocity of target 1, for all 7 time points. For the *scan-by-scan position and velocity RMSE*, we compare the track estimates with the classification given

in the third column of Table 3.5. Note that the classification is based on associating each state estimate to the target that last contributed a report to the track. The *scan-by-scan* and *global-mapping RMSE* computations are complementary approaches to understanding track accuracy.

4. SEISMIC TRACKING: EXPERIMENTAL RESULTS

Beyond what is listed in Table 3.2, our experimentation with seismic sensor involves the additional sensor specifications listed in Table 4.1.

Number of seismic sensors	4
Placement of seismic sensors	(75m, 75m), (-75m, 75m), (75m,-75m), (-75m,-75m)

Table 4.1. Seismic sensor placement.

The sensor locations and ranges, along with the region for target motion, are illustrated in Figure 4.1.

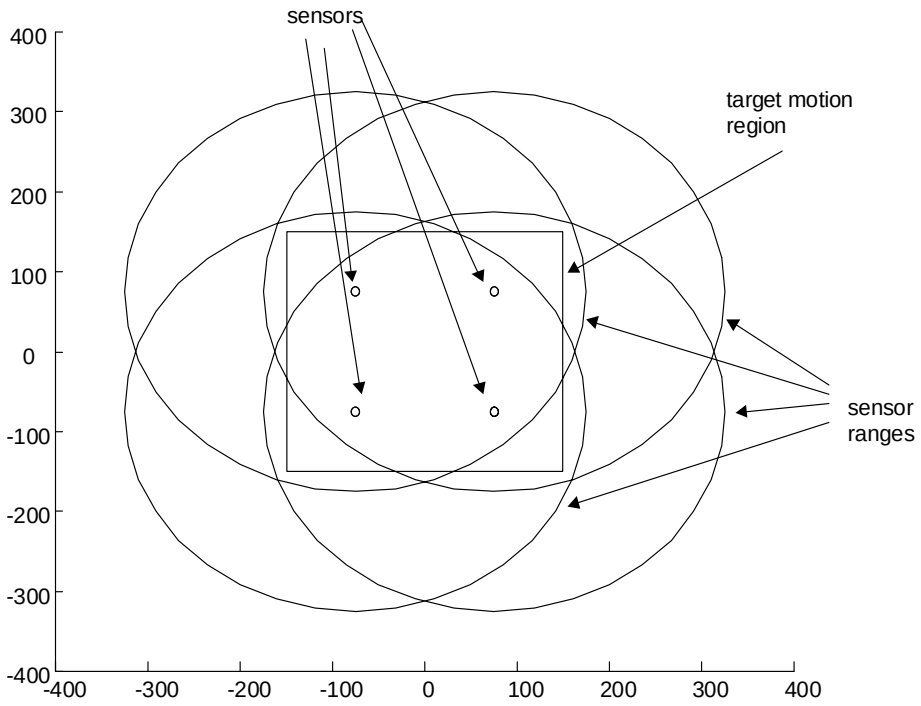

Figure 4.1. Scenario context.

Our experimentation with seismic sensors will focus on two important thresholds. The first is the threshold used in EKF/MHT processing to confirm tracks. The second is the detection threshold used to confirm target detections. As expected, there are tradeoffs in the selection of these thresholds in terms of tracking metrics of interest. First, we set the sensor detection probability and false alarm rates to the values listed in Table 4.2. A single stochastic realization of five target trajectories and sensor detections is shown in Figure 4.2. The experimental results given in Table 4.3 are based on 5 Monte Carlo runs, each of which includes 5 target trajectories.

Probability of detection	0.7
False alarm rate per unit area	$0.5 \cdot 10^{-6}\ \mathrm{m}^{-2}$

Table 4.2. Sensor parameters for the first set of experimental results.

Given the sensor range of 250m, the false alarm rate corresponds on average roughly to one false alarm per 10 scans of data. (For acoustic data, given the sensor range of 750m, this rate corresponds roughly to one false alarm per scan of data).

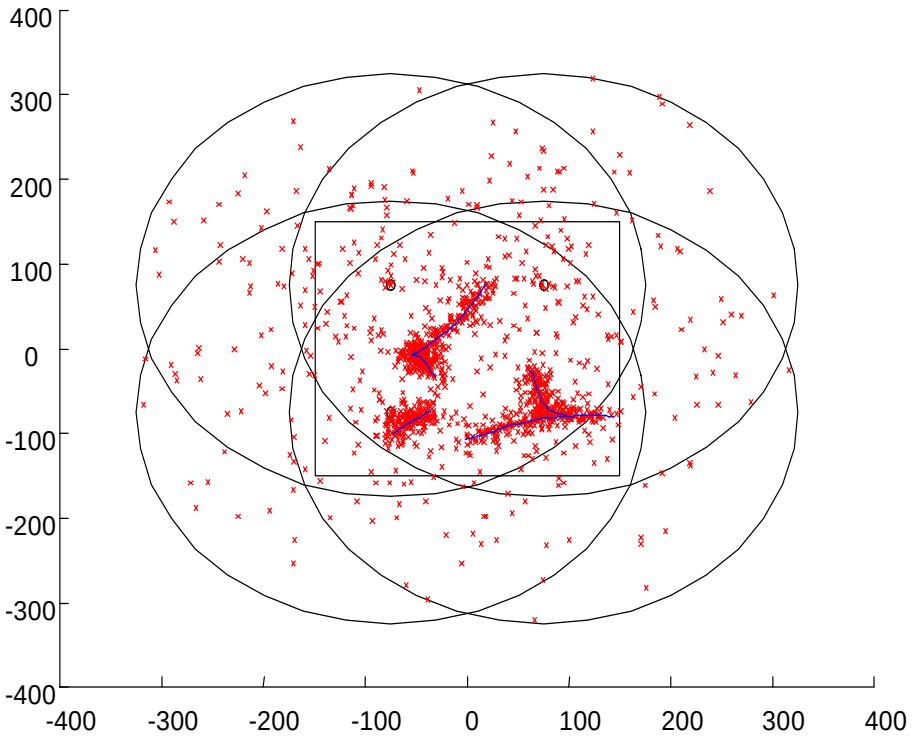

Figure 4.2. A stochastic realization of five target trajectories and sensor measurements.

Performance Metric	ξ = 2sec	ξ = 3sec	ξ = 4sec
Computation time	49.08	49.08	49.08
Percentage of false tracks	0.453	0.078	0.004
Fragmentation	8.216	3.800	3.064
Probability of correct association	0.942	0.947	0.950
Track life	1.181	1.144	1.118
Scan-by-scan position RMSE	8.535	7.688	7.224
Scan-by-scan velocity RMSE	1.177	1.159	1.145
Global-mapping position RMSE	8.230	7.353	6.849
Global-mapping velocity RMSE	1.145	1.126	1.111

Table 4.3. Seismic tracking performance as a function of confirmation threshold ξ.

Our results illustrate the impact of the choice of confirmation threshold on tracking performance. Note that *computation time* does not depend on the choice of threshold, since algorithmic processing is unaffected by its value. The key metrics that are impacted by the choice of threshold are the *percentage of false tracks* and the *fragmentation*, since most tracks that do not meet a higher confirmation threshold are false, and a higher threshold naturally reduces the number of confirmed tracks. The *probability of correct association* and *RMSE* metrics also improve as the confirmation threshold is raised. *Track life* remains consistently high: the total time duration of confirmed tracks consistently exceeds the actual time duration of the target trajectories. We would like the track life metric to be as close as possible to 1. As the confirmation threshold is increased further still, we find that the benefits in terms of track fragmentation and track precision are outweighed by a substantial decrease in track life, indicating that we are discarding relevant tracks with a too-stringent track confirmation threshold. Thus, in our subsequent experimentation we have fixed the confirmation threshold at 4sec.

Next, we examine the impact of the sensor detection threshold on algorithm performance. The results given in Table 4.4 are again based on 5 Monte Carlo runs, each with 5 target trajectories. Note that the middle column shows the previous results

(with the confirmation threshold at 4sec), while the results in the right column are based on simulations with a higher sensor detection threshold and higher false alarm rate: these correspond to a higher sensor detection threshold.

Performance Metric	$p_D = 0.7$ $\lambda_{FA} = 0.5 \cdot 10^{-6}\,\mathrm{m}^{-2}$	$p_D = 0.9$ $\lambda_{FA} = 0.5 \cdot 10^{-5}\,\mathrm{m}^{-2}$
Computation time	49.08	62.48
Percentage of false tracks	0.004	0.000
Fragmentation	3.064	1.520
Probability of correct association	0.950	0.981
Track life	1.118	1.048
Scan-by-scan position RMSE	7.224	5.445
Scan-by-scan velocity RMSE	1.145	1.046
Global-mapping position RMSE	6.849	5.151
Global-mapping velocity RMSE	1.111	1.023

Table 4.4. Seismic tracking performance as a function of the sensor detection threshold.

Note that, at the cost of an increase in computation time due to the increased number of sensor measurements with higher clutter, tracking performance is markedly improved with respect to all performance metrics. (As we noted earlier, track life should be close to 1). Thus, for effective tracking based on seismic data it appears crucial to have a good probability of detection, even at the cost of an increased false alarm rate. Indeed, the MHT approach effectively reasons over several scans of data so that the detrimental effect of increased clutter is mitigated.

5. ACOUSTIC TRACKING: EXPERIMENTAL RESULTS

A key issue in passive acoustic tracking is the limited observability of single sensors, due to their inability to measure range to the target [1]. The availability of an increasing number of dispersed sensors reduces the likelihood of an unfavorable geometry between sensors and targets, as well as providing an increased quantity of sensor data for more effective tracking. In addition, the combination of the MHT approach along with an increase in the number of sensors is critical in reducing ghosting effects, whereby a series of spurious triangulations may lead to the initiation and maintenance of an erroneous track. Of course, the increase in data leads to a corresponding increase in computational burden.

We compare the differences in tracking performance with two and four acoustic sensors. In the four-sensor case, the sensor locations are the same as in Tables 4.1. In the two-sensor case, the placement of the sensors is indicated in Table 5.1. Additional simulation parameters are given in Tables 3.1-3.3 and Table 5.1.

Placement of acoustic sensors	(75m, 0), (-75m, 0)
Probability of detection	0.7
False alarm rate per unit area	$1.0 \cdot 10^{-8}\,\mathrm{m}^{-2}$

Table 5.1. Acoustic sensor parameters (two-sensor case).

Note that we have set a lower false alarm rate per unit area than in the seismic data case. In part this is due to the larger acoustic sensor range, in part to the presence of some ghost tracks with higher false alarm rates, which complicates the interpretation of RMSE errors. Here, we are more interested in comparing performance as a function of the number of sensors, for relatively benign scenarios. Tracking performance in the two-sensor and four-sensor cases are given in Table 5.2. The results are based on 5 Monte Carlo runs, each of which is based on 3 target trajectories.

As in the experimental results with seismic data, we find that *global-mapping* RMSE errors are smaller than *scan-by-scan* RMSE errors. Here, the difference in the RMSE computations is accentuated due to the impact of incorrectly associated bearing-only detections in low-density target scenarios. As expected, in the two-sensor case we have decreased performance with respect to all tracking metrics, except for computation time since less sensor data is processed. In particular, the presence of ghost tracks significantly degrades the RMSE metrics.

Performance Metric	Two-sensor case	Four-sensor case
Computation time	24.37	38.05
Percentage of false tracks	0.000	0.000
Fragmentation	1.066	1.000
Probability of correct association	0.822	0.903
Track life	0.770	0.965
Scan-by-scan position RMSE	56.07	26.27
Scan-by-scan velocity RMSE	1.719	1.021
Global-mapping position RMSE	54.67	6.624
Global-mapping velocity RMSE	1.663	0.971

Table 5.2. Acoustic tracking performance as a function of the number of sensors.

In Figure 5.1, we illustrate a realization of ground target trajectories, sensor measurements, and tracks. Sensor measurements are indicated with a short line segment originating from the sensor. In general, we find that our ability to track targets accurately is reduced when target the overall sensor-to-target geometry is less favorable. In particular, when target move in the smaller region bounded by the four sensors, more accurate tracks are maintained.

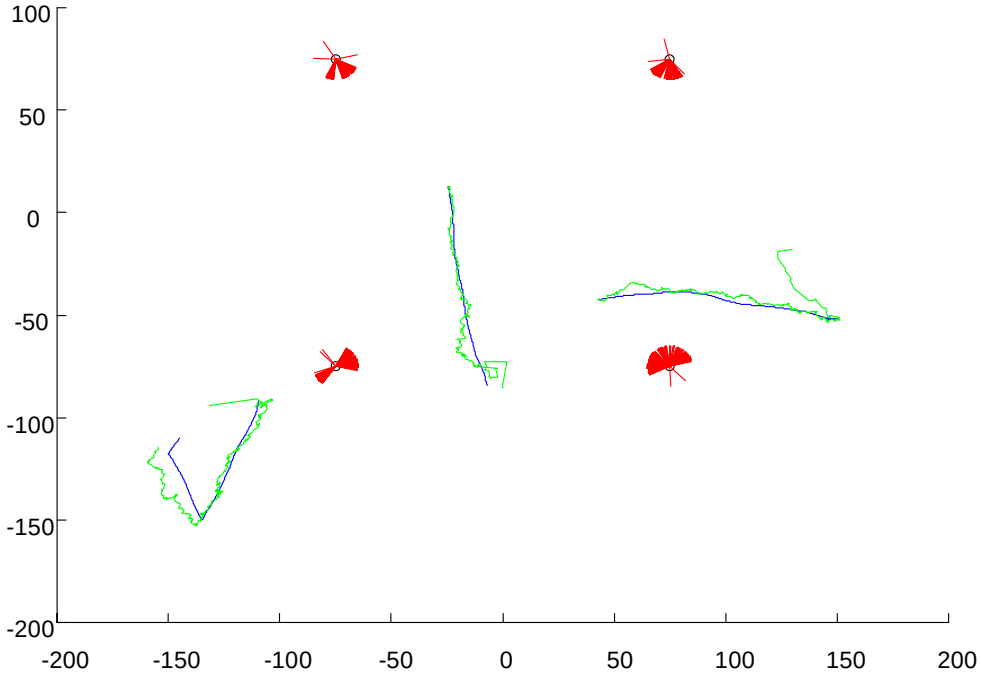

Figure 5.1. A stochastic realization of ground truth, acoustic sensor measurements, and acoustic tracks.

The impact of a less favorable geometry on tracking performance can be measured more directly by varying sensor placement. In particular, the next set of experimental results is based on bringing the four acoustic sensors close together, to a distance of 10m between neighboring sensors. Experimental results are given in Table 5.3 and are based on 5 Monte Carlo runs, each of which is based on three target trajectories. (The right column is the same as in Table 5.2).

Note that with close sensors, it is much more difficult to confirm tracks, as evidenced by a much lower track life and a fragmentation less than one, indicating that some targets trajectories do not lead to a confirmed track. The probability of correct association is also degraded, as are most of the RMSE quantities. Interestingly, computation time is much higher in the close-sensors case, due to the larger number of feasible associations that are created in MHT processing, as data association becomes less unambiguous.

Performance Metric	Unfavorable geometry	Favorable geometry
Computation time	63.19	38.05
Percentage of false tracks	0.000	0.000

Fragmentation	0.933	1.000
Probability of correct association	0.888	0.903
Track life	0.730	0.965
Scan-by-scan position RMSE	21.90	26.27
Scan-by-scan velocity RMSE	1.106	1.021
Global-mapping position RMSE	26.01	6.624
Global-mapping velocity RMSE	1.153	0.971

Table 5.3. Acoustic tracking performance as a function of sensor placement.

6. DIRECTIONS FOR FURTHER RESEARCH

In this paper, we have illustrated preliminary results based on an EKF/MHT approach to target tracking for simulated seismic and acoustic data. We have investigated the sensitivity of tracking performance on key parameters of the problem including the detection threshold associated with signal-level data, the number and location of sensors on the ground, and the track confirmation threshold. Our previous analysis of the scalability of our tracking algorithm [4] indicates the feasibility of processing data from much larger scenarios, with large numbers of sensors on the ground.

We plan to extend our work in a number of directions. First, we plan to enhance our sensor models to represent more faithfully their actual characteristics. In particular, we must clarify to what extent we can assume knowledge of the location and orientation of large number of inexpensive UGS that will not be GPS-equipped in general. This introduces an important registration and bias estimation aspect to the problem. Second, we plan to characterize and exploit additional feature information that is available from ground sensors, including amplitude and frequency information. Feature information is critical to effective multi-target tracking in dense target environments. Finally, we will continue to investigate enhancements to our baseline approach to tracking, including the use of enhanced IMM-based target motion models and filters [9][10] and the use of particle filtering techniques that have shown to perform well in highly nonlinear settings [11].

ACKNOWLEDGEMENT

This material is based on work supported by the Air Force Office of Scientific Research under Contract No. F49620-98-C-0010.

REFERENCES

1. S. Blackman and R. Popoli, *Design and Analysis of Modern Tracking Systems*, Artech House, 1999.
2. T. Kurien, Issues in the Design of Practical Multitarget Tracking Algorithms, in *Multitarget-Multisensor Tracking*, Y. Bar-Shalom (ed.), pp. 43-83, Artech House, 1990.
3. S. Coraluppi, C. Carthel, M. Luettgen, and S. Lynch, All-Source Track and Identity Fusion, in Proceedings of the *National Symposium on Sensor and Data Fusion*, June 2000, San Antonio TX, USA.
4. S. Coraluppi, C. Carthel, S. Lynch, and D. Herrick, All-Source Track and Identity Fusion: Recent Advances and Results, to appear in *Proceedings of the National Symposium on Sensor and Data Fusion*, June 2001, San Diego CA, USA.
5. Y. Bar-Shalom and X. Li, *Estimation and Tracking: Principles, Techniques, and Software*, Artech House, 1993 (reprinted by YBS Publishing, 1998).
6. Mazor, Averbuch, Bar-Shalom, and Dayan, Interacting Multiple Model Methods in Target Tracking: A Survey, *IEEE Transactions on Aerospace and Electronic Systems*, 34(1), 1998.
7. V. Aidala, Kalman Filter Behavior in Bearing-Only Tracking Applications, *IEEE Transactions on Aerospace and Electronic Systems*, Vol. 15(1), January 1979.
8. T. Song and J. Speyer, A Stochastic Analysis of a Modified Gain Extended Kalman Filter with Applications to Estimation with Bearing Only Measurements, *IEEE Transactions on Automatic Control*, Vol. 30(10), October 1985.
9. X. Li and Y. Bar-Shalom, Multiple-model estimation with variable structure, IEEE Transactions on Automatic Control, 41(4), 1996.
10. S. Coraluppi and C. Carthel, Multiple-Hypothesis IMM (MH-IMM) Filter for Moving and Stationary Targets, in *Proceedings of the 4th International Conference on Information Fusion*, August 2001, Montreal, Canada.
11. M. Mallick and T. Kirubarajan, Multi-sensor Single Target Bearing-only Tracking in Clutter, to appear in *Proceedings of the Meeting of the MSS Specialty Group on Battlefield Acoustic and Seismic Sensing, Magnetic and Electric Field Sensors*, October 2001, Laurel MD, USA.